Tidally Induced Ice Shell Fracturing and Faulting at Europa & Implications for Future Subsurface Missions

Rudi R. Lien[1,2] (rlien@uoregon.edu), Kate L. Craft[2], and Matt Walker[3]

[1]University of Oregon, Eugene, OR. [2]Johns Hopkins University Applied Physics Laboratory, Laurel, MD. [3]Planetary Science Institute, Tucson, AZ.

Introduction

- Tidal forcing on Europa's ice shell triggers fault-like motion along pre-existing surface fractures (1-2)
- Active faulting is a potential hazard for a probe and communication hardware during a subsurface mission (3)
- We model and quantify fracture slip resulting from tidal stresses for multiple:
  - Geographic locations
  - Fracture angles & orientations
  - Coefficient of friction values on fault plane
- Strain values that could potentially be imposed on a communication tether crossing an active fault are calculated from net fault displacement results

Model Set-up

- We use Ansys Mechanical to design a 3D pure ice block geometry (Fig. 1) and simulate tidal fracture slip based on calculated stress with depth (4)
  - Block sides fixed in X and Z directions
  - Block base fixed with tidal displacement data
- Fault plane added to block:
  - Extends to 900-m depth
  - 5, 20, or 45 degrees from vertical
  - North or east dipping
  - Coefficient of friction, μ: 0.1 or 0.55
- Tidal stresses & displacements are computed for two locations (Fig. 2):
  1. Subjovian (0°, 0°):
     - Vertical stress dominates
     - Location of maximum bulge
  2. Thera Macula chaos terrain (50°S, 180°E)
     - Lateral stress components dominate
     - Region of scientific interest for future missions (5)
- Fracture models are static (time-independent)
  - Tidal data are specific to Europa's perijove position, where maximum tidal bulging occurs

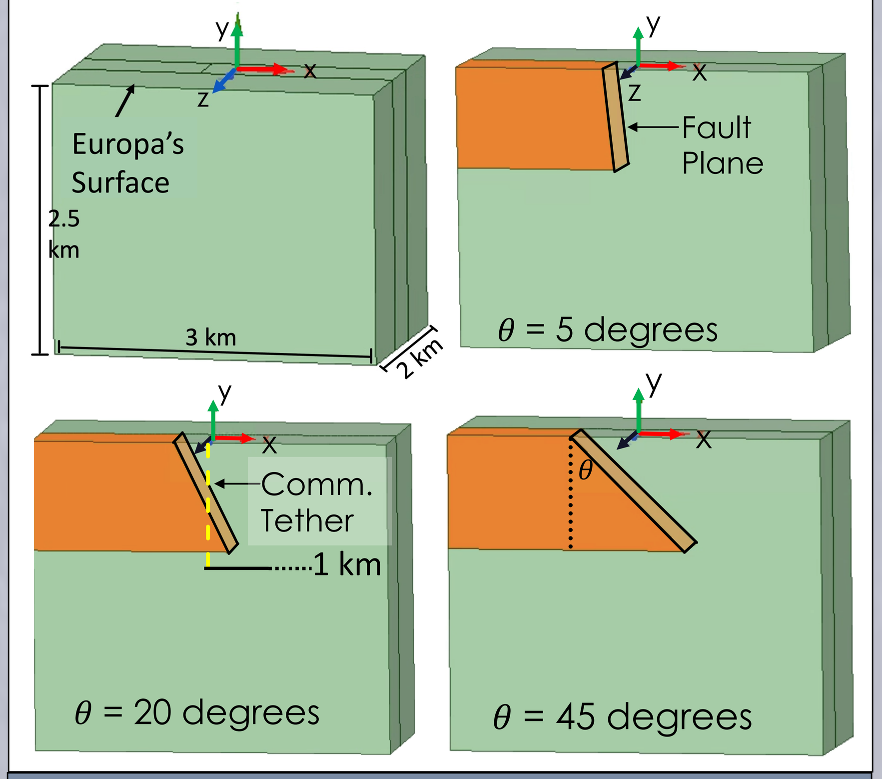

Figure 1. Ice block geometry (top left) and cross sections displaying each fracture angle θ. The +X direction represents either north or east, depending on the stress data set.

Ice Block Material Properties

Poisson's ratio: 0.30
Shear modulus: 3.5 GPa
Density: 920 kg/m^3
μ_{ice} (minimum) = 0.1
μ_{ice} (maximum) = 0.55

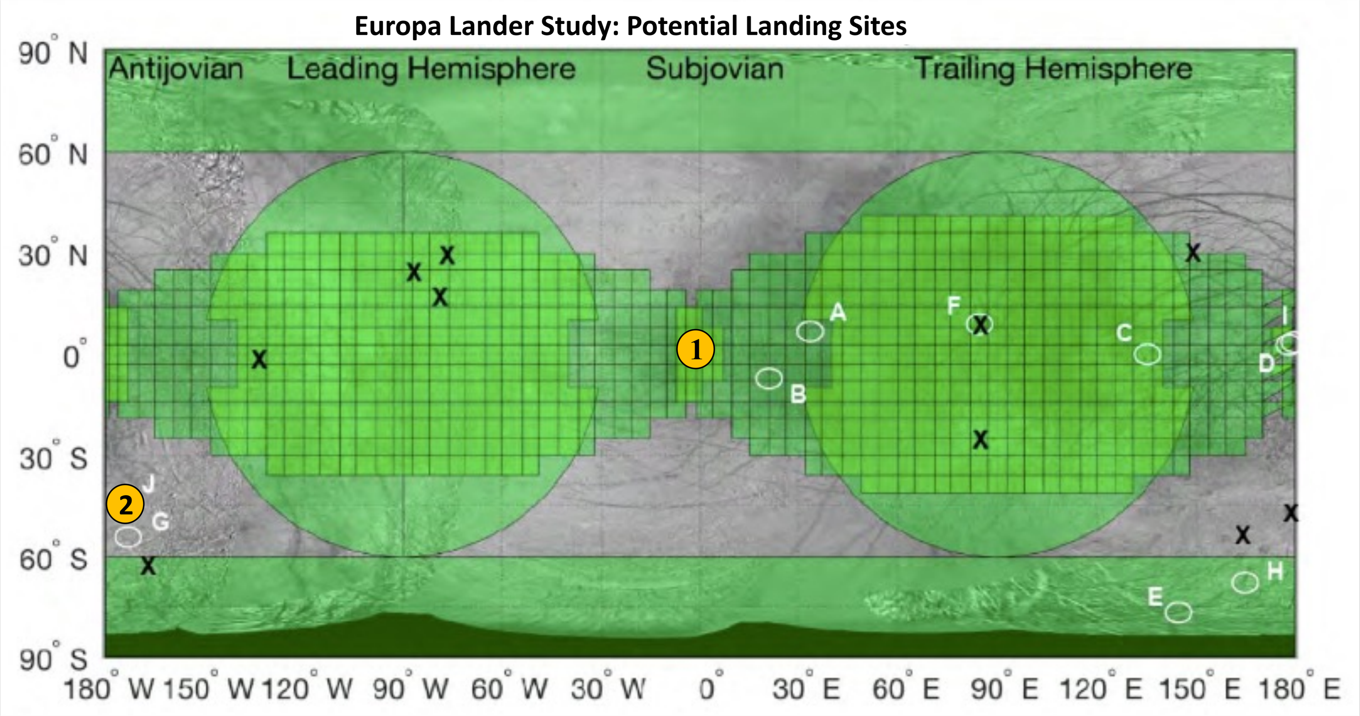

Figure 2. Adapted from (4). Orange circles were added to indicate the two locations selected for the fracture models presented here, 1) Subjovian and 2) Thera Macula chaos terrain. White circles and black x's are sites of scientific interest, while green shading represents areas unsuitable for landed missions.

Displacement & Strain Calculations

- Ansys Mechanical solves and outputs the X, Y, and Z directional deformation
- Net fault displacement magnitude, ||S||, is calculated as:

$$||S|| = \sqrt{X_{Def}^2 + Y_{Def}^2 + Z_{Def}^2}$$

- Maximum and minimum potential strain on a communication tether crossing a fault is calculated using ||S|| as the change in tether length

$$Strain = \frac{||S||}{l_0}$$

where l_0 is the original tether length

- For maximum strain, l_0 = 6.6 cm
  - Tether is stretched only locally
- For minimum strain, the tether is stretched across its entire length
  - We assume that the probe is at a depth of 1 km, so l_0 (min) = 1 km

Results

Subjovian – East dipping fracture

- Net fault displacement ranges from 0.2 – 4.3 cm
- Maximum displacement occurs at 700-750 m depth
- Fracture motion is independent of μ_{ice} due to opening rather than sliding of the fracture edges

Thera Macula (TM) – East dipping fracture

- Strike-slip motion for all fracture angles
- Change in direction of motion causes the increase in displacement magnitude at ~800 m
- Minor (<1 cm) differences caused by μ_{ice} (max vs. min)

5-degree fracture:

- Net fault displacement ranges from 4.9 – 8.1 cm
- Max displacement occurs at 475 m depth

20-degree fracture:

- Net fault displacement ranges from 12.2 – 36.9 cm
- Max displacement occurs at 525 m depth

45-degree fracture:

- Net fault displacement ranges from 10.8 – 61.9 cm
- Max displacement occurs at 570 m depth

Thera Macula – North dipping fracture

- Reverse fault motion for all fracture angles
- Displacement is larger with max μ_{ice} for 20- and 45-degree fractures by ~1 – 5 cm

5-degree fracture:

- Net fault displacement ranges from 17.9 – 81.5 cm
- Max displacement occurs at 400-450 m depth
- Max vs. min μ_{ice} causes up to 25.5 cm difference at the surface and decreases with depth

20-degree fracture:

- Net fault displacement ranges from 23.0 – 73.8 cm
- Max displacement occurs at 400-450 m depth

45-degree fracture:

- Net fault displacement ranges from 16.8 – 65.2 cm
- Max displacement occurs at ~500 m depth

Net Fault Displacement (cm)

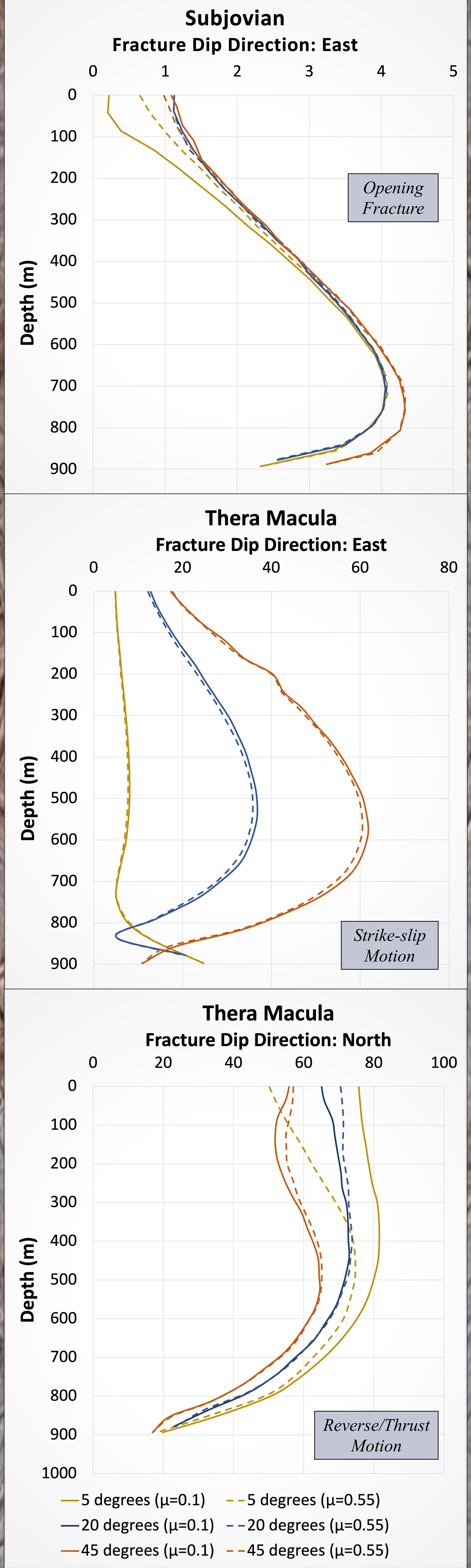

Tether Strain Analysis

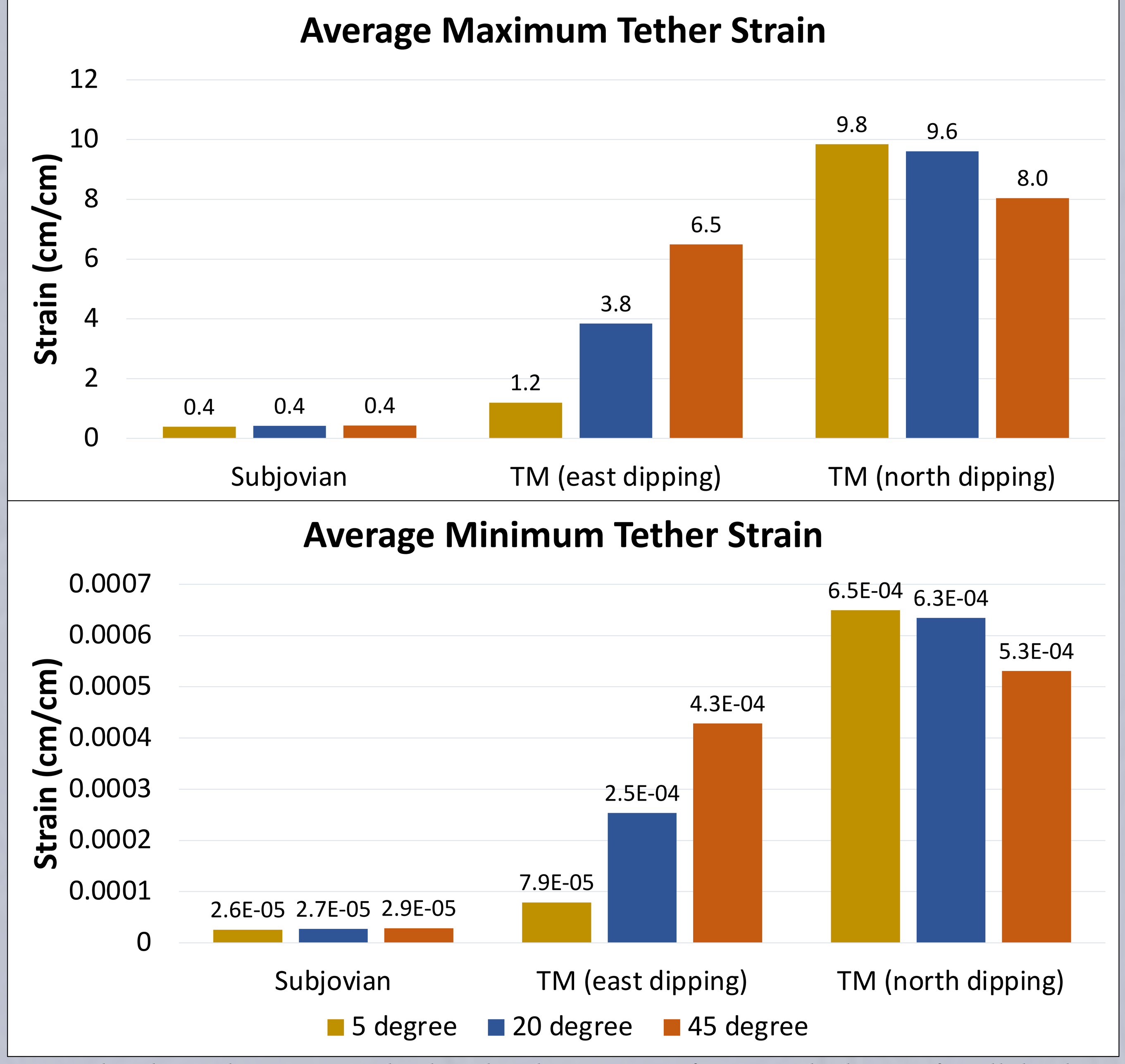

*In the above charts, strain displayed is the **average** of strain calculations for all depths (0-900 m) and the minimum and maximum μ_{ice} model outputs for each angle.*

Conclusions

- Net fault displacement varies considerably depending on fracture angle and orientation as well as geographic location on Europa
- The direction of fault slip is dependent on the stress vector, specifically whether lateral components are symmetrical, and dip direction of a fracture
- For the tether length used in maximum strain calculations, here assumed l_0 = 6.6 cm, maximum strain results for Thera Macula (east and north dipping fractures) exceed 100% length increase, which is not likely survivable for a comm. tether
  - Tether adhesion tests will be performed in follow-on COLDTech work to better understand the tether-ice adhesion properties and where strain would likely concentrate on these tethers
- Laboratory work by other STI members constrains the amount of strain an optical tether can tolerate under Europan conditions (6)

Ongoing Work

- We are working to model fracture slip over multiple time points throughout the tidal cycle
- Time-dependent models will indicate accuracy of static models as well as quantify accumulation of net displacement over each cycle
- Timestep models will allow us to determine a shear velocity and directly compare strain results to laboratory tested strain values (6)
- Tidal faulting models can be used to assess fracture hazards at future proposed landing sites

More on this work will be presented at GSA 2021 – Lien et al., Abs. #368590

Acknowledgements

We would like to acknowledge funding from the SESAME program, Grant #NNH18ZDA001N-SESAME, Montana Space Grant Consortium, and NASA SUPPR.

References

(1) Greenberg, R., et al. (1998) *Icarus*, 135, 64–78.
(2) Lee, S., Pappalardo, R. T., and Makris, N. C. (2005) *Icarus*, 177, 367–379.
(3) Craft et al. (2019) *AbSciCon*, Abs. 402-2.
(4) Walker et al. (2020) *51st LPSC*, Abs. 2448.
(5) Europa Lander Study 2016 Report: Europa Lander Mission. JPL D-97667.
(6) Singh et al. (2021) *AGU Fall Meeting*, submitted, Abs. 859271.